

**Comparative study of the initial spikes of SGR giant flares
in 1998 and 2004 observed with GEOTAIL:
Do magnetospheric instabilities trigger large scale fracturing of
magnetar's crust?**

Y. T. Tanaka¹, T. Terasawa², N. Kawai², A. Yoshida³, I. Yoshikawa¹, Y. Saito⁴,
T. Takashima⁴, and T. Mukai⁴

yasuyuki@eps.s.u-tokyo.ac.jp

ABSTRACT

We present the unsaturated peak profile of SGR 1900+14 giant flare on 1998 August 27. This was obtained by particle counters of the Low Energy Particle instrument onboard the GEOTAIL spacecraft. The observed peak profile revealed four characteristic structures: initial steep rise, intermediate rise to the peak, exponential decay and small hump in the decay phase. From this light curve, we found that the isotropic peak luminosity was 2.3×10^{46} erg s⁻¹ and the total energy was 4.3×10^{44} erg s⁻¹ ($E \gtrsim 50$ keV), assuming that the distance to SGR 1900+14 is 15 kpc and that the spectrum is optically thin thermal bremsstrahlung with $kT = 240$ keV. These are consistent with the previously reported lower limits derived from Ulysses and Konus-Wind observations. A comparative study of the initial spikes of SGR 1900+14 giant flare in 1998 and SGR 1806-20 in 2004 is also presented. The timescale of the initial steep rise shows the magnetospheric origin, while the timescale of the intermediate rise to the peak indicates that it originates from the crustal fracturing. Finally, we argue that the four structures and their corresponding timescales provide a clue to identify extragalactic SGR giant flares among short GRBs.

Subject headings: gamma rays: observation - stars: individual(SGR 1900+14) - stars: individual(SGR 1806-20) - stars: neutron - stars: magnetic fields - gamma rays: bursts

¹Department of Earth and Planetary Science, University of Tokyo, Japan

²Department of Physics, Tokyo Institute of Technology, Japan

³Department of Physics and Mathematics, Aoyama Gakuin University, Japan

⁴Japan Aerospace Exploration Agency, Japan

1. Introduction

Soft gamma-ray repeaters (SGRs) were first discovered as high-energy burst sources in the late 1970's (Mazets & Golenetskii 1981). Once SGRs enter burst active phases, they produce a lot of short-duration (~ 0.1 s) energetic ($\sim 10^{41}$ erg) soft gamma-ray bursts. These bursts were distinguished from cosmological gamma-ray bursts (GRBs) by the soft spectra and the repeated activities. Furthermore, as rare events, SGRs emit extremely bright giant flares (GFs). A GF lasts for several hundred seconds and its isotropic total energy amounts to $10^{44} - 10^{46}$ erg. So far, only three have been recorded. On 1979 March 5, the first GF was detected from SGR 0526-66 by Venera spacecraft (Mazets et al. 1979). The second GF was observed from SGR 1900+14 on 27 August 1998 (Hurley et al. 1999; Mazets et al. 1999; Feroci et al. 2001). Recently SGR 1806-20 emitted the third GF on 27 December 2004 (Terasawa et al. 2005; Hurley et al. 2005; Palmer et al. 2005; Mereghetti et al. 2005; Schwartz et al. 2005). The overall time profile of each GF is characterized by a very intense spectrally hard initial spike whose duration is $\lesssim 0.5$ s, and a subsequent pulsating tail which has a softer spectrum and lasts for some hundred seconds. After the GFs, radio afterglows were observed from SGR 1900+14 (Frail et al. 1999) and from SGR 1806-20 (Gaensler et al. 2005; Cameron et al. 2005).

SGRs show the slow spin periods (5 – 8 s) and rapid spin-down rates ($10^{-11} - 10^{-10}$ s s^{-1}) (Kouveliotou et al. 1998, 1999). Assuming magnetic dipole radiation, we can estimate the magnetic fields of SGRs to be $10^{14} - 10^{15}$ G and SGRs are recognized as magnetars (Duncan & Thompson 1992; Thompson & Duncan 1995, 1996). According to the magnetar model, the energy source of both recurrent bursts and GFs is the ultrastrong magnetic field: stored magnetic energy inside a magnetar is suddenly released via cracking of a magnetar's crust, and the large scale crustal fracturing produces GFs. Similar to earthquakes, the power-law distribution of the radiated energy of the repeated burst and the lognormal distribution of waiting times between successive bursts are reported (Cheng et al. 1996; Göğüş et al. 2000). These observations also support the idea that SGR bursts originate from the starquakes.

In this paper, first, we focus on the SGR 1900+14 GF on 1998 August 27. This flare was detected by gamma-ray instruments on the Ulysses, Konus-Winds and BeppoSAX satellites (Hurley et al. 1999; Mazets et al. 1999; Feroci et al. 2001). However the flare was so intense that these instruments underwent severe dead-time or pulse pile-up problems. Consequently, the time profile during the most intense period was not obtained and only the lower limits of the peak flux intensity and fluence were reported (Hurley et al. 1999; Mazets et al. 1999). Here we present the clear peak profile of the SGR 1900+14 GF on 1998 August 27. The profile was recorded by the Low Energy Particle instrument (hereafter LEP) (Mukai et al. 1994) onboard the GEOTAIL spacecraft, whose principal objective is to study the Earth's

magnetosphere. The light curve for the first 350 ms of the GF is unsaturated and has a high time resolution of 5.58 ms. We also show the energetics of the flare.

Second, we present a comparative study of the initial spikes of SGR GFs in 1998 and 2004, the latter of which was also detected by the same instrument (Terasawa et al. 2005). From both of the light curves, we extract the characteristics of the initial spikes of SGR GFs, focusing on the timescales discovered during the initial spikes. Finally we argue that the observed timescales may provide a clue to identify extragalactic SGR giant flares among short GRBs.

2. Instrumentation and Observation

The LEP is designed to measure three-dimensional velocity distributions of the Earth’s magnetospheric ions and electrons. It consists of two nested sets of quadspherical electrostatic analyzers; one analyzer to select ions, and the other to select electrons. At the receiving end of the ion and electron optics, seven microchannel plate detectors (MCPs) and seven channel electron multipliers (CEMs) are used, respectively. During the SGR 1806-20 GF in 2004, the peak flux was so intense that the MCPs were saturated during the first 150 ms. Alternatively the peak profile was derived from the CEMs, because the CEMs are much less sensitive to gamma-rays than the MCPs. After the most intense period, the MCPs recovered from the saturation and observed the decay profile clearly. On the other hand, during the SGR 1900+14 GF in 1998, we obtained the peak profile from the MCPs. The peak flux of the 1998 GF was about one-tenth of that of the 2004 GF (see below), and hence the MCPs did not suffer the severe saturation problem. The CEMs showed count increases ($\lesssim 20$) corresponding to those of the MCPs. However, since the background electron counts for CEMs were high ($\sim 50-80$), we do not use the CEM data for the analysis of the SGR 1900+14 GF.

The LEP records the data every 15/8192 of the spacecraft spin period over 32 sequences, followed by a gap of 1/256 of the spin period. The spacecraft spin period was 3.046 s on 1998 August 27, leading to $3.046 \times (15/8192) = 5.58 \times 10^{-3} \text{ s} = 5.58 \text{ ms}$ time resolution. This is slightly different compared to a 5.48 ms time resolution of SGR 1806-20 GF observation in 2004, during which the spin period was 2.993 s.

In this report, we use the LEP calibration that the effective energy range and the detection efficiency are $> \sim 50 \text{ keV}$ and $\sim 1\%$ against incident photons, respectively. Since the LEP was not designed to measure gamma-rays, this calibration was made after the launch of the GEOTAIL spacecraft through the analyses of solar flare photons for which the

Hard X-ray Telescope onboard the Yohkoh satellite (Kosugi et al. 1991) provided photon energy spectra and intensities. Recently we have made (i) GEANT4 simulations based on the detailed mass model of the LEP, satellite structure and other instruments, and (ii) the laboratory measurements of the detection efficiency of the MCP (Tanaka et al. 2007), both of which have successfully reproduced what were obtained from the solar flare photon analyses. In addition, we found from the GEANT4 simulations that the effect of the rotation of the spacecraft was negligibly small around the spin phase angles corresponding to the two GFs.

Fig. 1 shows the first 350 ms unsaturated peak profile of the GF from SGR 1900+14 on 27 August 1998. Dead time and saturation effects are negligible for the count rates smaller than ~ 1000 counts per 5.58 ms: only the peak count at $t=5.58$ ms was dead-time corrected. The shaded bars in Fig. 1 indicate the instrumental data gaps of 12 ms. The onset time ($t=0$) was 10:22:15.47 UT, which coincided with the expected arrival time at the GEOTAIL position. Before the onset, the count was less than 25 counts per 5.58 ms (shown by a black arrow in Fig. 1(b)), i.e. the background level. Then it increased to 792 counts within 5.58 ms, and this rapid increase provided the upper limit of the e-folding time of the initial rise as 1.6 ms. After the onset, it reached a very sharp peak of 4776 counts at $t=5.58$ ms. This increase yielded the e-folding time of the intermediate rise time to the peak as $3.1^{+0.9}_{-2.0}$ ms. Following the peak, it decayed rapidly. The exponential decay time was calculated as 2.9 ± 0.2 ms from the counts for $t=5.6-22$ ms. Note that the timing of the dip at $t=22$ ms corresponds to the timing of the temporal count recovery from the total shut down of the Konus-Wind instrument (see Fig. 6 of Mazets et al. (1999)). After that, it increased again with e-folding time of 16 ± 2.5 ms for $t=22-50$ ms and reached a flat-top second peak during 60–120 ms. Finally the exponential decay was clearly observed and the decay time was obtained as 23 ± 1.6 ms during $t=120-160$ ms. Note that a small hump was seen around 310 ms, which was also observed with the Konus-Wind instrument (Fig.6 of Mazets et al. (1999)).

To convert physical quantities such as an energy flux from the observed count rates, we need an assumption on the photon energy spectrum, because the LEP detected integrated photon numbers above 50 keV. We assume $kT=240$ keV optically thin thermal bremsstrahlung (OTTB) spectrum which was obtained from Ulysses observation (Hurley et al. 1999). Resultant physical quantities are tabulated in Table 1, combined with Venela observation of the SGR 0526-66 GF in 1979 (Mazets et al. 1999) and GEOTAIL observation of the SGR 1806-20 GF in 2004 (Terasawa et al. 2005). We found that the peak luminosity and the total emitted energy are $2.3 \times 10^{46} d_{15}^2$ erg s $^{-1}$ and $4.3 \times 10^{44} d_{15}^2$ erg ($E \gtrsim 50$ keV), respectively. Here we assume that the distance to SGR 1900+14 is 15 kpc (Vrba et al. 2000) and $d_{15} = (d/15\text{kpc})$. We also found that the total energy of this GF is about 130 times smaller than that of the 2004 December 27 GF from SGR 1806-20, although it is reported

that the energy emitted during the pulsating tail in each GF is comparable ($E_{\text{tail}} \sim 10^{44}$ erg, see Table 1). (Hurley et al. 2005; Palmer et al. 2005; Mazets et al. 1999). Note that this difference by a factor of 130 is the same order of the radio observations: the radio afterglow of the SGR 1900+14 GF is approximately 500 times fainter than that of the SGR 1806-20 GF (Frail et al. 1999; Gaensler et al. 2005; Cameron et al. 2005).

3. Discussion

We observed two SGR GFs out of ever recorded three: from SGR 1900+14 in 1998 and SGR 1806-20 in 2004. Here we present a comparative study and extract characteristics of the initial spikes of the SGR GFs. Fig. 1 and Fig. 2 show the light curves of the initial spikes of SGR 1900+14 GF and SGR 1806-20 GF, respectively. Fig. 3 shows the detailed initial rise profiles of both GFs. From these light curves, we identify four common features: (1) initial steep rise (2) intermediate rise to the peak (3) exponential decay (4) small hump in the decay phase. The calculated e-folding times corresponding to the structures of (1)-(3) and the timing when we observed the structure (4) are tabulated in Table 1.

First, we focus on (1) initial steep rise. The observed initial rise time of SGR 1900+14 GF is ≤ 1.6 ms. This is comparable to the initial rise time of ≤ 1.3 ms observed in the SGR 1806-20 GF, implying the same physical mechanism producing the initial rapid energy release of these two GFs. Note that in the leading edge of the initial spike of SGR 1806-20 GF, Swift and Rhesi observed the similar timescale (Swift: ~ 0.3 ms, Rhesi: 0.38 ± 0.04 ms) (Palmer et al. 2005; Boggs et al. 2006). These correspond to our observation of ≤ 1.3 ms initial rise time. According to the reconnection model of GFs (Thompson & Duncan 1995; Duncan 2004), reconnection typically occurs at a fraction of the Alfvén velocity (Thompson & Duncan 1995; Duncan 2004), and this interpretation leads to $\tau_{\text{mag}} \sim L/0.1V_A \sim 0.3(L/10\text{km})$ ms, where L is the scale of the reconnection-unstable zone, and $V_A \sim c$ is the Alfvén velocity in the magnetosphere. This theoretical timescale τ_{mag} seems consistent with the observation of the initial rise time.

Next, we consider (2) intermediate rise to the peak. The observed e-folding rise time of the SGR 1900+14 GF is 3.1 ms, which is shorter than the 9.4 ms rise time observed in the SGR 1806-20 GF by factor of about 3.0. If this timescale is limited by the propagation of a fracture, we can infer the fracture size l as $l \sim 4\text{km}(t_{\text{rise}}/4\text{ms})$ (Thompson & Duncan 2001). Using this, the fracture size of the SGR 1900+14 is estimated as ~ 3.1 km, and that of the SGR 1806-20 is as ~ 9.4 km. It should be noted that our 9.4 ms rise time observed in the SGR 1806-20 GF differs by factor of ~ 2 from 4.9 ms derived from the CLUSTER spacecraft observation of the same GF (Schwartz et al. 2005). The origin of the difference between these

time scales is not understood, but could possibly attribute to the different energy coverages of the detectors. Unfortunately, since the energy response of the CLUSTER detectors against incoming X-ray and gamma-ray photons was not calibrated, further quantitative comparison between GEOTAIL and CLUSTER is not possible.

In the initial spike of the SGR 1900+14 GF in 1998, we found a deep dip and rebrightening following a sharp peak (Fig. 1). We propose that this dip explains the temporal recovery of the counter of the Konus-Wind (Mazets et al. 1999), since the dip and the recovery occurred nearly simultaneously. Note that Swift and Rhesi also detected a dip and rebrightening in the leading edge of the initial spike of the SGR 1806-20 GF (Palmer et al. 2005; Boggs et al. 2006), which could not be resolved by the GEOTAIL observation. This association implies that the dip and rebrightening are common features of the initial spikes of the SGR GFs, although theoretical interpretation is unclear.

Then, we concentrate on (3) exponential decay. The decay time of the SGR 1900+14 GF is 23 ms. This is shorter than the 66 ms decay time of the SGR 1806-20 GF by factor of 2.9, which roughly coincides with the factor 3.0 found in the intermediate rise times. From this similarity, we infer that the decay time is also proportional to the fracture size of a magnetar’s crust.

Finally, we focus on (4) small hump in the decay phase. Small humps are observed nearly at the same timing; ~ 310 ms in 1998 and ~ 430 ms in 2004 (note that the hump in 2004 GF was also observed with Swift satellite (Palmer et al. 2005)), although the total emitted energy differs by a factor of 130. This implies that the hump is caused by the continuing energy injections rather than the environmental interactions of the flare ejecta.

To conclude, the observed initial rise times imply that the onsets of both of the GFs result from magnetospheric instabilities. The intermediate rise times, on the other hand, are consistent with the idea that main energy release mechanism of the GFs is the large scale crustal fracturing. For this interpretation to be valid, magnetospheric instabilities should trigger the cracking of a magnetar’s crust. Further theoretical study is needed.

The above four structures discovered in the initial spikes may provide a clue to identify extragalactic SGR GFs among short GRBs. Recently, a possible detection of an extragalactic SGR GF is reported (Golenetskii et al. 2005). Bright short GRB 051103 was localized near the M81/M82 galaxy group by the interplanetary network. This association implies that the GRB 051103 is the SGR GF outside the local group. Furthermore, if the GRB 051103 is emitted from a SGR in M81, the isotropic total energy amounts to $\sim 7 \times 10^{46}$ erg, which is the same order of the energy of SGR 1806-20 GF (Frederiks et al. 2006). Not only existence of star forming regions inside the IPN error quadrilateral of GRB 051103 but also no detection

of optical and radio afterglow support the SGR hypothesis (Ofek et al. 2006). Here we investigate the hypothesis from the viewpoint of its light curve.

(1) The light curve of GRB 051103 observed by Konus-Wind showed a steep rise and the timescale is reported as ≤ 6 ms (Frederiks et al. 2006). This nearly corresponds to the intermediate rise time of a galactic SGR GF presented above, although we do not know whether the timescale observed by Konus-Wind represents an initial rise time or an intermediate rise time. Furthermore, (2) quasi-exponential decay was seen and the decay time is ~ 55 ms (Frederiks et al. 2006). This timescale is also the same order of magnitude as the decay times presented above. These two similarities found in the light curves also support the SGR hypothesis. A hump in a decay phase was not seen in the light curve of GRB 051103. This is explicable in terms of the detector’s detection limit, because the flux of the humps, if exists, are expected to be about one hundredth of the peak flux.

We thank R. Yamazaki for valuable comments and discussions. We are also grateful to all the members of GEOTAIL team for their collaboration. Y.T.T. is receiving a financial support from JSPS.

REFERENCES

- Boggs et al. 2006, astro-ph/0611318
- Cameron et al. 2005, Nature, 434, 1112
- Cheng et al. 1996, Nature, 382, 518
- Duncan, R. C. 2004, in Cosmic explosions in three dimensions, ed. P. Höflich, P. Kumar, & J. C. Wheeler, 285–+
- Duncan, R. C., & Thompson, C. 1992, ApJ, 392, L9
- Feroci et al. 2001, ApJ, 549, 1021
- Frail et al. 1999, Nature, 398, 127
- Frederiks et al. 2007, Astronomy Letters, 33, 19
- Gaensler et al. 2005, Nature, 434, 1104
- Golenetskii et al. 2005, GRB Coordinates Network, 4197, 1

- Gögüş et al. 2000, ApJ, 532, L121
- Hurley et al. 2005, Nature, 434, 1098
- Hurley et al. 1999, Nature, 397, 41
- Kosugi et al. 1991, Sol. Phys., 136, 17
- Kouveliotou et al. 1998, Nature, 393, 235
- Kouveliotou et al. 1999, ApJ, 510, L115
- Mazets et al. 1999, Astronomy Letters, 25, 635
- Mazets, E. P., & Golenetskii, S. V. 1981, Ap&SS, 75, 47
- Mazets et al. 1979, Nature, 282, 587
- Mereghetti et al. 2005, ApJ, 624, L105
- Mukai et al. 1994, J. Geomag. Geoelectr., 46, 669
- Ofek et al. 2006, ApJ, 652, 507
- Palmer et al. 2005, Nature, 434, 1107
- Schwartz et al. 2005, ApJ, 627, 129
- Tanaka et al. 2007, Review of Scientific Instruments, 78, 034501
- Terasawa et al. 2005, Nature, 434, 1110
- Thompson, C., & Duncan, R. C. 1995, MNRAS, 275, 255
- . 1996, ApJ, 473, 322
- . 2001, ApJ, 561, 980
- Vrba et al. 2000, ApJ, 533, L17
- Woods, P. M., & Thompson, C. 2004, astro-ph/0406133

Table 1: Comparison of three SGR giant flares

	SGR 1900+14	SGR 1806-20	SGR 0526-66
Initial Spike			
E-folding initial rise time [ms]	< 1.6	< 1.3	< 2
E-folding intermediate rise time [ms]	$3.1^{+0.9}_{-2.0}$	9.4 ± 1.1	-
Exponential decay time [ms]	23 ± 1.6	66 ± 12	~ 40
Timing of Small hump [ms]	~ 310	~ 430	-
Peak photon flux [photons $\text{cm}^{-2} \text{s}^{-1}$]	$(3.2^{+4.0}_{-1.1}) \times 10^6$	$(2.5^{+1.1}_{-0.6}) \times 10^7$	-
Peak flux [erg $\text{cm}^{-2} \text{s}^{-1}$]	$0.85^{+1.0}_{-0.30}$	19^{+9}_{-4}	1×10^{-3}
Peak luminosity [erg s^{-1}]	$(2.3^{+2.7}_{-0.8}) \times 10^{46} d_{15}^2$	$(5.1^{+2.3}_{-1.2}) \times 10^{47} d_{15}^2$	$3.6 \times 10^{44} d_{55}^2$
Fluence [erg cm^{-2}]	$(1.6^{+2.0}_{-0.6}) \times 10^{-2}$	$2.0^{+0.9}_{-0.5}$	4.5×10^{-4}
Total Energy [erg]	$(4.3^{+5.3}_{-1.5}) \times 10^{44} d_{15}^2$	$(5.4^{+2.4}_{-1.3}) \times 10^{46} d_{15}^2$	$1.6 \times 10^{44} d_{55}^2$
Energy range	$E \gtrsim 50 \text{ keV}$	$E \gtrsim 50 \text{ keV}$	$E > 30 \text{ keV}$
Pulsating Tail			
Tail Energy [erg]	$1.2 \times 10^{44} d_{15}^2$	$1.2 \times 10^{44} d_{15}^2$	$3.6 \times 10^{44} d_{55}^2$
Energy range	$E > 15 \text{ keV}$	$3 < E < 100 \text{ keV}$	$E > 30 \text{ keV}$
Reference	1	2, 3	1

References. — (1) Mazets et al. 1999; (2) Terasawa et al. 2005; (3) Hurley et al. 2005

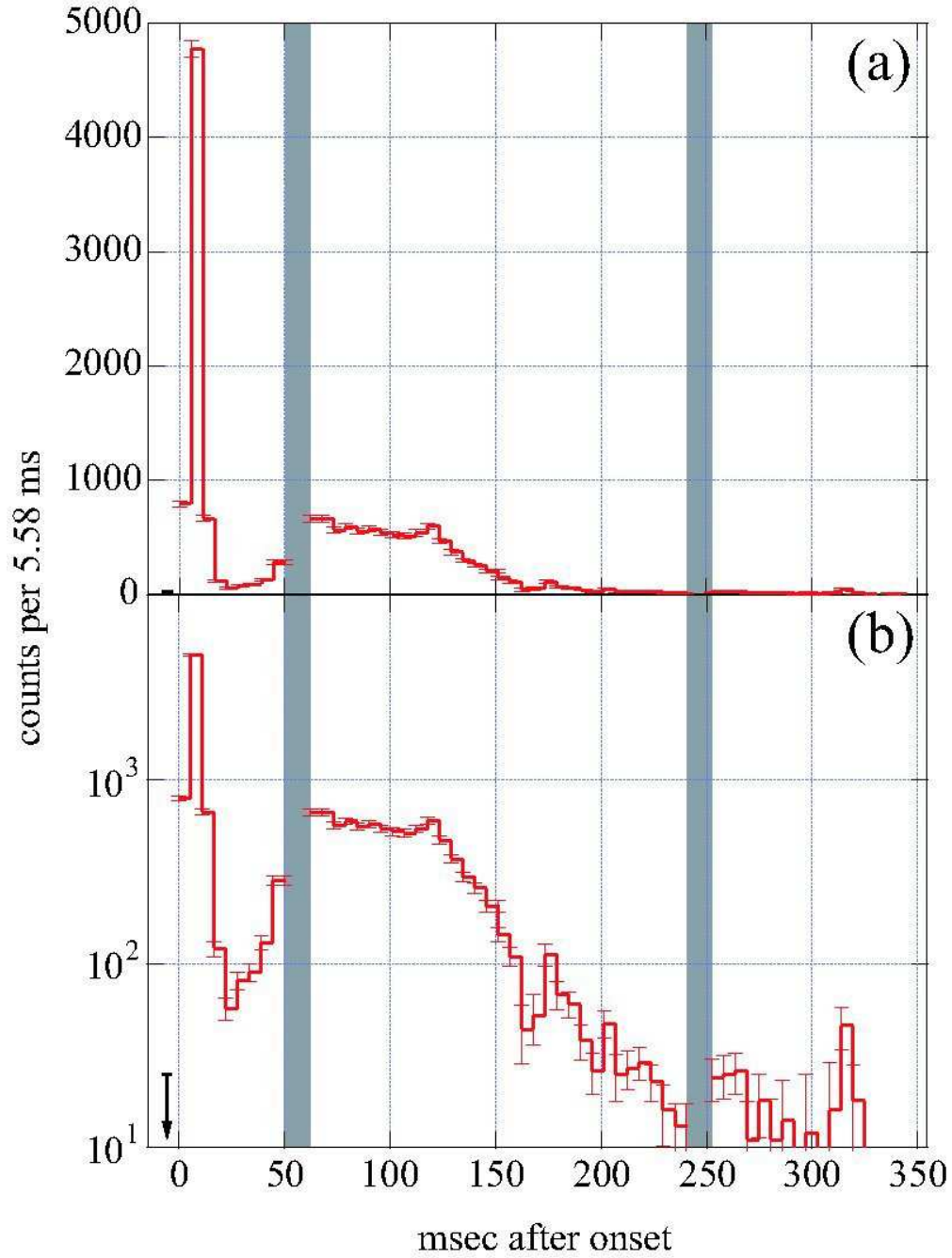


Fig. 1.— The first 350 ms unsaturated peak profile of the SGR 1900+14 GF observed with GEOTAIL (a) linear scale, and (b) log scale. The time resolution is 5.58 ms and the energy range is $E \gtrsim 50$ keV. Shaded bars indicate the instrumental data gaps of 12 ms.

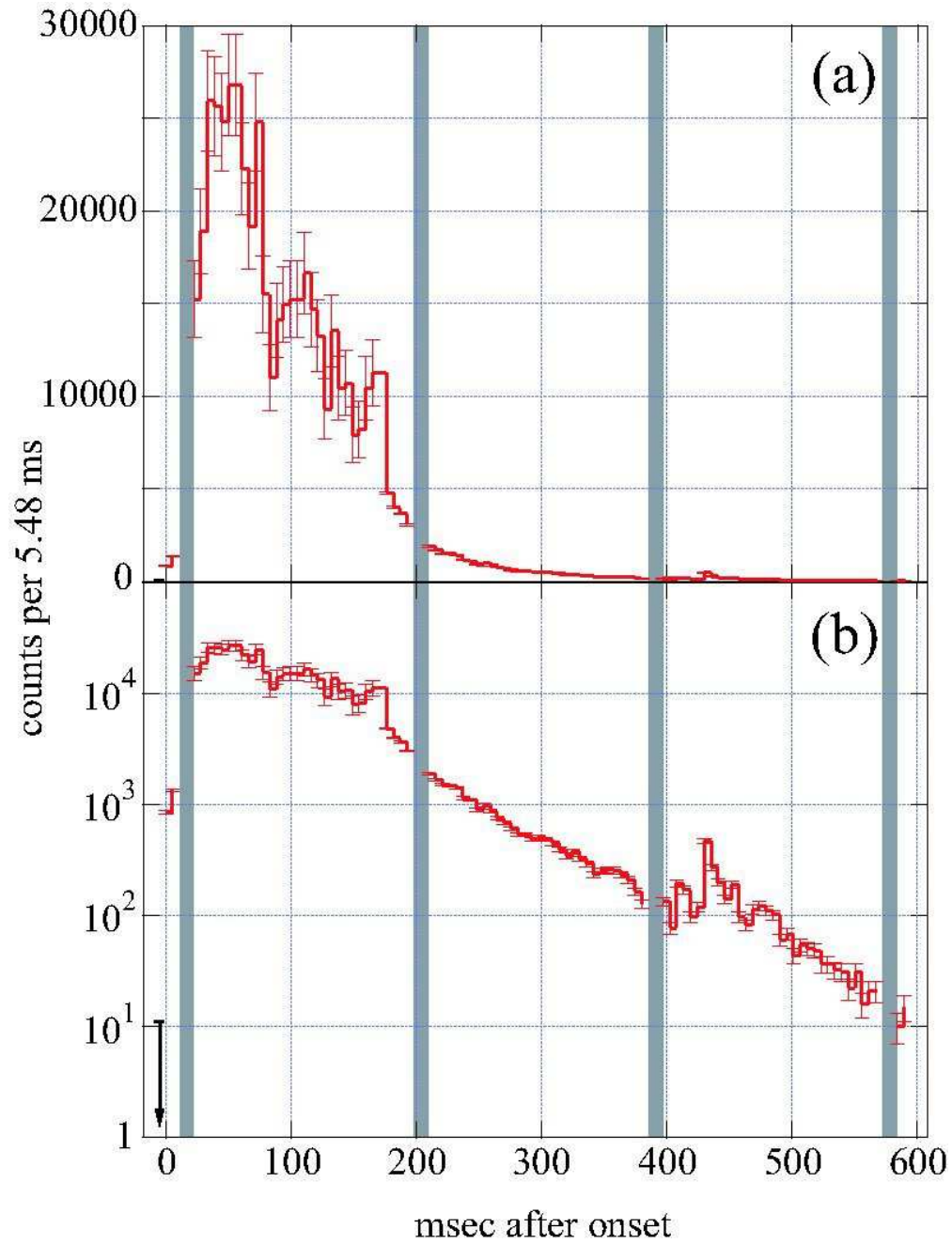


Fig. 2.— The $E \gtrsim 50$ keV gamma-ray time profile of the initial spike of SGR 1806-20 GF on 2004 December 27 observed with GEOTAIL (a) linear scale, and (b) log scale (Terasawa et al. 2005). The time resolution is 5.48 ms. Shaded bars indicate the instrumental data gaps of 12 ms.

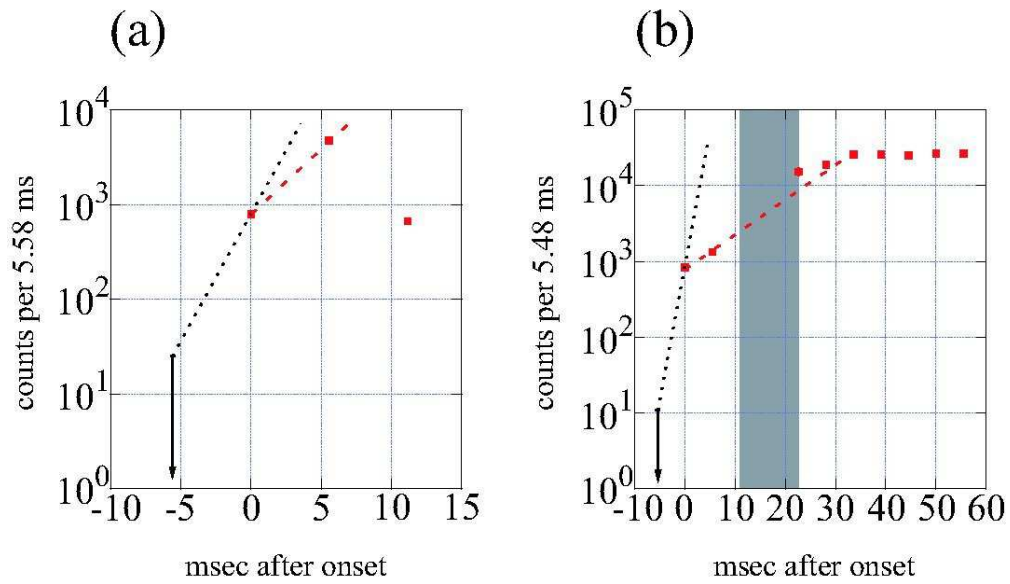


Fig. 3.— Detailed initial rise profiles of the initial spikes of (a) SGR 1900+14 GF in 1998, and (b) SGR 1806-20 GF in 2004. The vertical axes are log scale. Two different e-folding rise times are clearly seen in both of the initial spikes. The arrow shows the upper limit of photon counts before the onset.